Time-dependent quantum trajectories and thermodynamics

Christopher Kitching

10134621

School of Physics and Astronomy

The University of Manchester

Fourth Year
MPhys Project

May 2021

This project was performed in collaboration with *Elanor Harrington*

Abstract

The aim of this project is to further develop the idea of open quantum systems: a quantum mechanical system in contact with environmental degrees of freedom. Last semester, we studied such systems through the mathematical framework of density operators and master equations. We focused on a numerical method for calculating the density matrix by stochastically averaging many simulated trajectories of the systems wave-function with time, called the quantum trajectories or quantum jump method. In this project we aim to take our analysis further by generalising to a time-dependent Hamiltonian and investigating the adiabatic and diabatic limits in different bases. Specifically we look at Landau-Zener style transitions where the Hamiltonian varies such that the energy separation of the states is a linear function of time, in which case there exists analytic solutions for comparison in the absence of an environment. After introducing an environment we explore how changing its parameters alters our results. Ultimately this leads to a study of thermodynamic properties such as heat, work and entropy in different regimes and their relevance in areas such as quantum computation.

1. Introduction

Open quantum systems consist of a system and external environment, interactions between which significantly alter the dynamics. To understand these systems we require an alternative mathematical framework than the unitary operators which are used to treat closed systems. Previously we discussed the concept of density matrices, originally introduced by John von Neumann in 1927 [1], which can describe any state, pure or mixed, along with their effective equations of motion, known as master equations. In most scenarios analytic solutions don't exist and numerical solutions are demanding [2, p; 60]. To get around this, we utilise a method known as the quantum trajectory method, originally introduced by Castin and Mølmer in the early 1990s [3], which reduces the complexity in exchange for a stochastic average. We focus here on two-level systems which are simple to work with but have a wide range of applications in areas such as atomic physics or quantum computation.

In general, our Hamiltonian may contain a time-dependence which complicates the method slightly. An interesting case to consider is that of a Landau-Zener style transition where the time-dependence of the Hamiltonian corresponds to a linear increase in the separation energy of our two states. The speed at which we change such energy determines whether we observe transitions in different bases; an analytic formula for the probability of such transitions was published separately by Lev Landau [4] and Clarence Zener [5] in 1932 in the case of no environment. The introduction of an environment adds in the possibility for quantum jumps to occur which significantly changes the dynamics and requires taking a stochastic average over many trajectories. Parameters such as regime speed, temperature and coupling strength play a key role in how the properties of our system evolve.

We begin by recapping the mathematical formalism of density operators and Markovian master equations along with a brief outline of the quantum trajectories method. We then turn to studying adiabatic dynamics in the context of Landau-Zener transitions for the z-basis and energy-basis. Initially we exclude the environment, in which case we can compare to analytic solutions, and later re-introduce it; exploring how its parameters affect our results. In the later half of the report we turn to study thermodynamic properties such as work, heat and entropy and how they change under different regimes. Specifically, we look at applications to quantum computing through quantum logic gates and investigate what conditions are needed to replicate the effects of these gates, namely heat costs and the amount of work we are required to do.

2. Theoretical background

Before studying time dependence or thermodynamics, which are the focus of this report, we look to recap the necessary background theory. Namely, master equations and the numerical method of quantum trajectories used to unravel them and subsequently calculate properties of our system.

2.1. Markovian master equations in Lindblad form

When dealing with open quantum systems, we use an object known as the density operator, $\rho(t)$, which encodes all information about the system [6, p; 99]. It generalises the notion of the

wave-function to mixed states, which are what we work with here due to the statistical ensembles. For a system characterised by an ensemble of states, $\{|\psi_i(t)\rangle\}$, the density operator takes its most general form [7, p; 111]

$$\rho(t) \equiv \sum_i \rho_i \left|\psi_i(t)\right\rangle \left\langle\psi_i(t)\right|, \tag{2.1.1}$$

where ρ_i is the probability that the system realises the pure quantum state $|\psi_i(t)\rangle$. The population of a state $|x\rangle$, denoted ρ_{xx}, can be extracted by taking the trace of said state with the density operator

$$\rho_{xx}(t) = \langle x| \rho(t) |x\rangle . \tag{2.1.2}$$

The equation of motion for the density operator is known as the Liouville von-Neumann equation [7, p; 111]

$$\frac{\partial}{\partial t}\rho(t) = -i[H(t), \rho(t)], \tag{2.1.3}$$

where $H(t)$ is the Hamiltonian of our system, and in general contains a time-dependence.

It is useful to transform from the current Schödinger picture, where we hold the operators constant in time and allow our states to evolve, to the interaction picture, where we partition our full Hamiltonian, H, as

$$H = H_0 + H_I \tag{2.1.4}$$

where H_0 is chosen to be exactly solvable and H_I contains more complex terms. Operators are converted to the picture via the unitary transformation [8, p; 388]

$$\tilde{O}(t) = U_0^\dagger(t, t_0) O(t) U_0(t, t_0), \tag{2.1.5}$$

where the tilde notation represents an operator in the interaction picture and $U(t, t_0)$ is a unitary operator, which for a time-dependent Hamiltonian has the general form [9, p; 3]

$$U(t, t_0) = \underset{\leftarrow}{T} \exp\left[-i \int_{t_0}^{t} ds H(s)\right], \tag{2.1.6}$$

where $\underset{\leftarrow}{T}$ is the time-ordering operator. Equation (2.1.5) highlights the usefulness of this representation as we have effectively absorbed the easily soluble part of the Hamiltonian into the definition of our operators, leaving only the complex interaction part, which can be treated as a perturbation. The evolution of the density operator in the interaction picture, analogously to equation (2.1.3), also has Liouville von-Neumann form

$$\frac{\partial \tilde{\rho}(t)}{\partial t} = -i[\tilde{H}(t), \tilde{\rho}(t)], \tag{2.1.7}$$

where these operators have been transformed into the interaction picture by means of equation (2.1.5).

In what follows we actually need only work with the reduced density operator defined as [10, p; 259]

$$\rho_S(t) = Tr_E(\rho(t)), \tag{2.1.8}$$

where we have used the partial trace operator to "trace out" the environmental degrees of freedom. This object has dimensions much less than the full density operator while retaining all information about the system.

Now we wish to solve equation (2.1.7) by performing an initial integration, substituting back into the original equation and then taking the partial trace, leaving

$$\frac{\partial \tilde{\rho}_S(t)}{\partial t} = -iTr_E[\tilde{H}_I(t), \tilde{\rho}(0)] - \int_0^t ds \, \mathrm{Tr}_E \left[\tilde{H}_I(t), [\tilde{H}_I(s), \tilde{\rho}(s)]\right]. \tag{2.1.9}$$

From here, several simplifying assumptions are made [11, pp; 12-13]:

1. At $t = 0$ there are no correlations between the system and the environment.
2. The environment is assumed to be thermal and consequently the trace term of equation (2.1.9) can be shown to be zero for linear coupling.
3. The Born approximation extends assumption (1) to all times provided the coupling is weak.
4. The Markov approximation makes the equation memoryless provided the environment memory time is short compared to the timescale for system evolution.

After applying these assumptions, equation (2.1.9) can be written in the form

$$\frac{\partial \tilde{\rho}_S(t)}{\partial t} = -\int_0^\infty d\tau Tr_E \left[\tilde{H}_I(t), [\tilde{H}_I(t-\tau), \tilde{\rho}_S(t) \otimes \rho_E]\right]. \tag{2.1.10}$$

Taking this further requires a specific form of Hamiltonian. We choose the form of the interaction Hamiltonian to be

$$H_I = \sum_\alpha A_\alpha \otimes B_\alpha, \tag{2.1.11}$$

where A_α and B_α are the system and environment operators respectively, and then transform this to the interaction picture using equation (2.1.5) to get

$$\tilde{H}_I(t) = \sum_\alpha \tilde{A}_\alpha(t) \otimes \tilde{B}_\alpha(t), \tag{2.1.12}$$

where $\tilde{A}_\alpha(t) = e^{iH_S t} A_\alpha e^{-iH_S t}$ and $\tilde{B}_\alpha(t) = e^{iH_E t} B_\alpha e^{-iH_E t}$. We also introduce environment correlation functions [9, p; 31]

$$C_{\alpha\beta}(t,s) = \left\langle \tilde{B}_\alpha(t)\tilde{B}_\beta(s)\right\rangle_E = Tr(\tilde{B}_\alpha(t)\tilde{B}_\beta(s)\rho_E), \tag{2.1.13}$$

where we have used the fact that an expectation of an operator can be written as its trace with the density operator [9, p; 11]

$$\left\langle \hat{O}\right\rangle = Tr\left(\hat{O}\rho\right). \tag{2.1.14}$$

In the case of a stationary environment, i.e $[H_E, \rho_E] = 0$, it can easily be shown that

$$C_{\alpha\beta}(t,s) = Tr_E(\tilde{B}_\alpha(t-s)B_\beta\rho_E) \equiv C_{\alpha\beta}(t-s). \tag{2.1.15}$$

Expanding out the commutators of equation (2.1.10), substituting in our decomposed Hamiltonian (2.1.12) and using the environment correlation functions (2.1.15) we get the interaction picture master equation

$$\frac{\partial \tilde{\rho}_S(t)}{\partial t} = -\sum_{\alpha\beta}\int_0^\infty d\tau \left(\left[\tilde{A}_\alpha(t), \tilde{A}_\beta(t-\tau)\tilde{\rho}(t)\right] C_{\alpha\beta}(\tau) + \left[\tilde{\rho}_S(t)\tilde{A}_\beta(t-\tau), \tilde{A}_\alpha(t)\right] C_{\beta\alpha}(-\tau)\right). \tag{2.1.16}$$

The context of this report will focus on modelling a 2-level system coupled to a bath of bosonic oscillators. Physically this could represent, for example, a spin-$\frac{1}{2}$ particle that can flip between states interacting with a thermal environment. Such a scenario is encapsulated within the spin-boson model, whose total, time dependent, Hamiltonian can be written as [12, p; 3]

$$H_{\text{tot}} = \frac{\epsilon(t)}{2}\sigma_z + \frac{\Delta(t)}{2}\sigma_x + \sum_{\mathbf{k}} \omega_{\mathbf{k}} b_{\mathbf{k}}^\dagger b_{\mathbf{k}} + \sigma_z \sum_{\mathbf{k}} g_{\mathbf{k}}(b_{\mathbf{k}}^\dagger + b_{\mathbf{k}}). \tag{2.1.17}$$

The first two terms define the system Hamiltonian, H_{sys}, where $\epsilon(t)$ is the energy splitting and $\Delta(t)$ is the tunnelling coefficient accounting for the tunnelling between states. The matrices σ_z and σ_x are the Pauli matrices defined to be [6, pp; 65, 69]

$$\begin{aligned} \sigma_z &= |\uparrow\rangle\langle\uparrow| - |\downarrow\rangle\langle\downarrow|, \\ \sigma_x &= |\uparrow\rangle\langle\downarrow| + |\downarrow\rangle\langle\uparrow|, \end{aligned} \tag{2.1.18}$$

where $|\uparrow\rangle$ and $|\downarrow\rangle$ are the states of our two-level system in a basis set by σ_z. The third term is the environment Hamiltonian, where $\omega_{\mathbf{k}}$ is the frequency of the harmonic oscillators, and $b_{\mathbf{k}}^\dagger$ and $b_{\mathbf{k}}$ are the bosonic creation and annihilation operators respectively. Finally, the fourth term is that of the interaction, where $g_{\mathbf{k}}$ are coupling constants.

Although it is possible to work in the basis set by σ_z, for the quantum trajectories method it is convenient, and more physically motivated, to work in the eigen-basis set by the system Hamiltonian, which we will denote by $|+\rangle$ and $|-\rangle$. The transformation to the energy eigen-basis can be shown to be

$$\begin{aligned} |+\rangle &= \sin\left(\frac{\theta(t)}{2}\right)|\downarrow\rangle + \cos\left(\frac{\theta(t)}{2}\right)|\uparrow\rangle, \\ |-\rangle &= \cos\left(\frac{\theta(t)}{2}\right)|\downarrow\rangle - \sin\left(\frac{\theta(t)}{2}\right)|\uparrow\rangle, \end{aligned} \tag{2.1.19}$$

where $\theta(t) = \tan^{-1}\left(\frac{\epsilon(t)}{\Delta(t)}\right)$, and therefore $\cos\theta(t) = \frac{\epsilon(t)}{\eta(t)}$ and $\sin\theta(t) = \frac{\Delta(t)}{\eta(t)}$, where $\eta(t) = \sqrt{\epsilon(t)^2 + \Delta^2(t)}$.

We now transform the interaction part of the Hamiltonian in equation (2.1.17) to the interaction picture and consequently find that

$$\tilde{A}(t) = P_0 - \left(P_\eta^\dagger e^{i\eta t} + P_\eta e^{-i\eta t}\right), \tag{2.1.20}$$

$$\tilde{B}(t) = \sum_{\mathbf{k}} g_{\mathbf{k}} \left(b_{\mathbf{k}}^\dagger e^{i\omega_{\mathbf{k}} t} + b_{\mathbf{k}} e^{-i\omega_{\mathbf{k}} t}\right), \tag{2.1.21}$$

where

$$P_0(t) = \frac{\epsilon(t)}{\eta(t)}\left(|+\rangle\langle+| - |-\rangle\langle-|\right), \tag{2.1.22}$$

$$P_\eta(t) = \frac{\Delta(t)}{\eta(t)}|-\rangle\langle+|. \tag{2.1.23}$$

We see that $P_\eta(t)$ changes the state entirely whereas $P_0(t)$ is simply a phase change. We then substitute (2.1.20) and (2.1.21) into equation (2.1.16) and evaluate the commutators. The environment correlation functions, defined by equation (2.1.13), also need to be explicitly evaluated and we find we can take a continuum limit to write

$$C(\pm\tau) = \int_0^\infty d\omega J(\omega) \left[N(\omega) e^{\pm i\omega\tau} + (1 + N(\omega)) e^{\mp i\omega\tau} \right]. \tag{2.1.24}$$

$N(\omega)$ is the Bose-Einstein occupation number defined by [9, p; 2]

$$N(\omega) = \left(e^{\frac{\omega}{k_B T}} - 1 \right)^{-1}, \tag{2.1.25}$$

where T is the bath temperature and k_B is the Boltzmann constant. $J(\omega)$ is the spectral density defined by [13, p; 7]

$$J(\omega) = \sum_{\mathbf{k}} |g_{\mathbf{k}}|^2 \delta(\omega - \omega_{\mathbf{k}}), \tag{2.1.26}$$

which describes the density of the bath modes weighted by the square of their individual coupling strength to the system. Finally, we make what is known as the secular approximation where we ignore fast oscillating terms by assuming that their contributions are small when the typical timescale for system evolution is short compared to the environment relaxation time [14]. Ultimately we arrive at, transforming back to the Schrödinger picture, the secular master equation

$$\begin{aligned} \frac{\partial \rho(t)}{\partial t} = -i[H_s(t) + H_{LS}, \rho_S(t)] &+ \Gamma_0 \left(P_0(t)\rho_S(t)P_0(t) - \frac{1}{2}\{P_0^2(t), \rho_S(t)\} \right) \\ &+ \Gamma(t)(1 + N(t)) \left[P_\eta(t)\rho_S(t)P_\eta^\dagger(t) - \frac{1}{2}\{P_\eta^\dagger(t)P_\eta(t), \rho_S(t)\} \right] \\ &+ \Gamma(t)N(t) \left[P_\eta^\dagger(t)\rho_S(t)P_\eta(t) - \frac{1}{2}\{P_\eta(t)P_\eta^\dagger(t), \rho_S(t)\} \right]. \end{aligned} \tag{2.1.27}$$

The H_{LS} term is a Lamb-shift term that is usually ignored as it it typically negligible and can always be absorbed into the parameters $\epsilon(t)$ and $\Delta(t)$. The terms Γ_0 and $\Gamma(t)$ are terms proportional to the rates in the corresponding channels. For a simple ohmic spectral density of the form $J(\omega) = \alpha\omega$, where α is the system-bath coupling strength, we can write them as

$$\Gamma_0 = 2\pi \lim_{\omega \to 0} J(\omega)(1 + N(\omega)) \approx 4\pi\alpha k_B T, \tag{2.1.28}$$

$$\Gamma(t) = 2\pi J(\eta) = 2\pi\alpha\eta(t). \tag{2.1.29}$$

The secular approximation that we made earlier requires that $\eta \gg \Gamma$ which imposes upper limits on α that must be obeyed to remain in a weak coupling regime.

2.2. Quantum trajectories method

The quantum trajectories technique is a numerical method used to unravel master equations in Lindblad form and obtain the density matrix [15]. It has advantages in reducing the dimensions

of the problem and provides some intuitive insight. One of its major advantages is that the process can be parallelised, since trajectories are independent, which we utilise for the calculations in this report. We will briefly recap the idea behind the method before implementing it.

In general, Markovian master equations, specifically our secular master equation in (2.1.27), working in dimensionless units, have Lindblad form [7]

$$\frac{\partial \rho_S(t)}{\partial t} = -i[H(t), \rho_S(t)] - \frac{1}{2}\sum_m \Gamma_m (c_m^\dagger c_m \rho_S(t) + \rho_S(t) c_m^\dagger - 2 c_m \rho_S(t) c_m^\dagger), \tag{2.2.1}$$

where c_m are the Lindblad operators, or jump operators, that describe dissipative dynamics that occur at characteristic rates Γ_m. This equation can be re-written as [16, p; 86]

$$\frac{\partial \rho_S(t)}{\partial t} = -i(H_{\text{eff}} \rho_S(t) - \rho_S(t) H_{\text{eff}}^\dagger) + \sum_m \Gamma_m c_m \rho_S(t) c_m^\dagger, \tag{2.2.2}$$

where the effective Hamiltonian, H_{eff}, is defined as [16, p; 86]

$$H_{\text{eff}} = H_S - \frac{i}{2}\sum_m \Gamma_m c_m^\dagger c_m. \tag{2.2.3}$$

Equation (2.1.27) is of Lindblad form and thus the effective Hamiltonian can be read off as

$$\begin{aligned} H_{\text{eff}} = \frac{\epsilon(t)}{2}\sigma_z + \frac{\Delta(t)}{2}\sigma_x - \frac{\Gamma_0}{2}P_0(t)^2 \\ - i\frac{\Gamma(t)}{2}\left(1 + N(t)\right) P_\eta^\dagger(t) P_\eta(t) - i\frac{\Gamma(t)}{2} N(t) P_\eta(t) P_\eta^\dagger(t). \end{aligned} \tag{2.2.4}$$

This effective Hamiltonian can then be used in the quantum trajectories algorithm to propagate a state forward in time. The principle of the algorithm is to propagate the state under the effective Hamiltonian to determine a candidate state. The norm of this new state then determines whether a quantum jump occurs, in which case we act with the appropriate jump operator, or if not, the final state is proportional to the candidate state [16, pp; 88-89]. Thus working in the energy-basis is intuitive as if the initial state is chosen as either $|+\rangle$ or $|-\rangle$ it will remain as such until a quantum jump occurs. The details of the algorithm and its equivalency to solving the master equation were detailed in last semesters report.

Note that throughout we will always use a time-step $dt = 0.1$ for simulation length $t_{\max} \geq 20$, otherwise we use a time-step a factor of 200 smaller than $t_{\max}$. This is the largest, and therefore least computationally expensive, time-step that does not cause the algorithm to break down

3. Adiabatic dynamics

We have now re-capped the concept of open-quantum systems, the mathematical formalism of master equations and the method of quantum trajectories used to unravel them. Now we turn to studying time-dependence, specifically we study Hamiltonians where the energy separation of the states is a linear function of time.

3.1. Quantum adiabatic theorem

Consider first the case with no environment, where the system Hamiltonian has a simple form that depends on a time dependent detuning

$$H_S = \frac{\epsilon(t)}{2}\sigma_z = \frac{\epsilon(t)}{2}\left(|\uparrow\rangle\langle\uparrow| - |\downarrow\rangle\langle\downarrow|\right), \tag{3.1.1}$$

The eigenstates of our system Hamiltonian, $|\uparrow\rangle$ and $|\downarrow\rangle$, have energies $\frac{\epsilon(t)}{2}$ and $-\frac{\epsilon(t)}{2}$ respectively. For reasons that will become clear, we will name these states the diabatic states. Clearly if we prepare the system in one of these states it will remain in that state forever. In the special case that $\epsilon(t) = 0$ there is a two fold degeneracy and the system will remain in any prepared state. Figure (1) shows the energies of these two states and we see that the energy of $|\uparrow\rangle$ increases linearly with $\epsilon(t)$ while that of state $|\downarrow\rangle$ decreases linearly with $\epsilon(t)$.

Now we add in a tunneling term to our system Hamiltonian which allows the system to switch between eigenstates. The tunnelling coefficient is chosen to be a constant and thus the system Hamiltonian reads

$$H = \frac{\epsilon(t)}{2}\sigma_z + \frac{\Delta}{2}\sigma_x. \tag{3.1.2}$$

Now the Hamiltonian eigenstates have changed to what we denote as $|+\rangle$ and $|-\rangle$ with energies which can be easily derived as

$$\frac{\eta_\pm(t)}{2} = \pm\frac{1}{2}\sqrt{\epsilon^2(t) + \Delta^2}. \tag{3.1.3}$$

These new states will be known as the adiabatic states. Figure (1) also shows the energies of these two new states varying with $\epsilon(t)$ as two branches of a hyperbola, with the upper branch representing $|+\rangle$ and the lower representing $|-\rangle$. At $\epsilon(t) = 0$ the separation of these hyperbola is, Δ. For non-zero values of the tunnelling coefficient the eigenvalues of the Hamiltonian cannot be degenerate, thus we see a phenomena known as an avoided crossing.

Now, the adiabatic theorem states that a physical system prepared in its instantaneous eigenstate will remain in that state, if the given perturbation is acting slowly enough and there is a gap between the eigenvalue and the rest of the Hamiltonian's spectrum [17]. So if we consider a case with $\Delta \neq 0$, starting in the $|-\rangle$ state with negative $\epsilon(t)$, where $|\epsilon(t)| \gg \Delta$ (the far left side of the solid red curve shown in the right hand image of Figure (1)), then increasing $\epsilon(t)$ adiabatically i.e. $\frac{d\epsilon(t)}{dt} \to 0$, to a positive $\epsilon(t)$, where $|\epsilon(t)| \gg \Delta$, will ensure that the system remains in that eigenstate of the Hamiltonian and will thus follow the solid red curve in the right hand image of Figure (1). Alternatively, a diabatic increase of $\epsilon(t)$, i.e. $\frac{d\epsilon(t)}{dt} \to \infty$, will ensure we follow the diabatic path (the dashed red line shown in the right hand image of Figure (1)), such that the basis states flip. In the middling case, where $0 < \frac{d\epsilon(t)}{dt} < \infty$, there is a finite probability to find the system in either of its eigenstates. How to calculate such probabilities is outlined in Sub-section (3.2).

We can now use the quantum trajectories method to demonstrate the above idea by utilising two different bases, the z/diabatic-basis and the energy/adiabatic-basis. We fix the tunnelling coefficient, $\Delta = 0.01$, and vary the detuning, $\epsilon(t) \in [-10, 10]$, as shown in Figure (2).

Since we are not considering the effect of the environment we only need a single trajectory. We start in the state $|-\rangle$ with negative $\epsilon(t)$, where $|\epsilon(t)| \gg \Delta$, so that the states $|-\rangle$ and $|\uparrow\rangle$ are

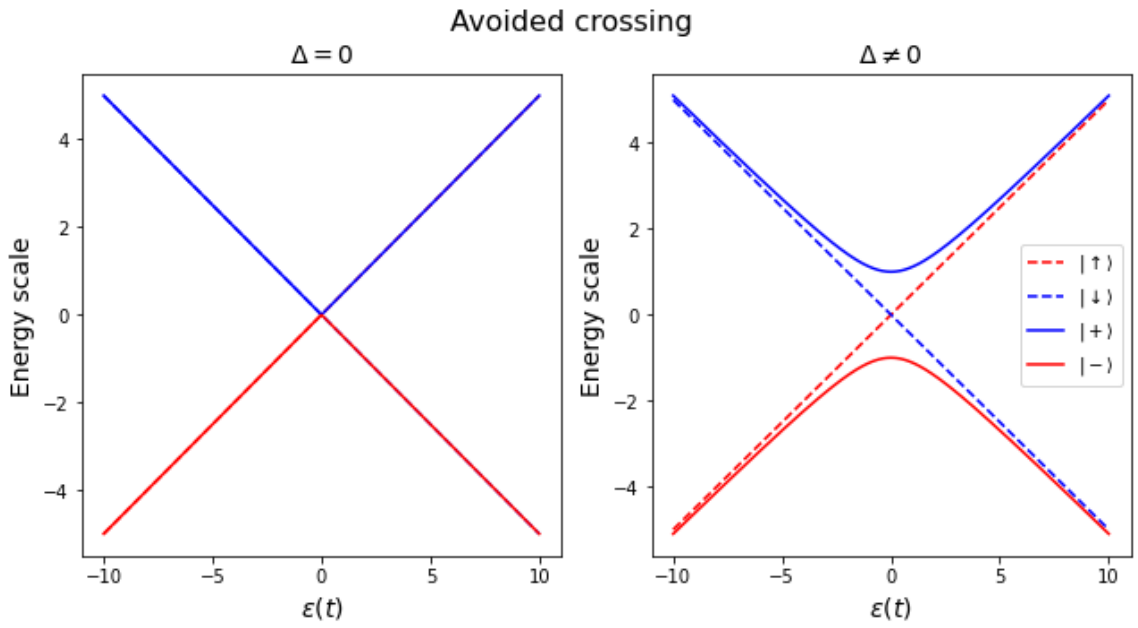

Figure 1: Two plots showing the eigen-energies of different states increasing with the detuning, $\epsilon(t)$. The diabatic states (red and blue dashed lines) are shown to have linearly increasing and decreasing energies. The adiabatic states (red and blue solid lines) have hyperbolic form. The left hand plot shows the case where $\Delta = 0$ and there is no difference between the adiabatic states and the diabatic states. Note the adiabatic states (solid lines) lie directly on top of the diabatic states (dashed lines) and so are not visible in this plot. Additionally, at $\epsilon(t) = 0$ we observe a two-fold degeneracy in both the adiabatic and diabatic states. The right plot shows the case of a finite tunnelling coefficient, $\Delta \neq 0$, where only the diabatic states have a degeneracy at $\epsilon(t) = 0$, while the adiabatic states demonstrate the avoided crossing. For values of $|\epsilon(t)| \gg 1$ the diabatic and adiabatic states are approximately equal.

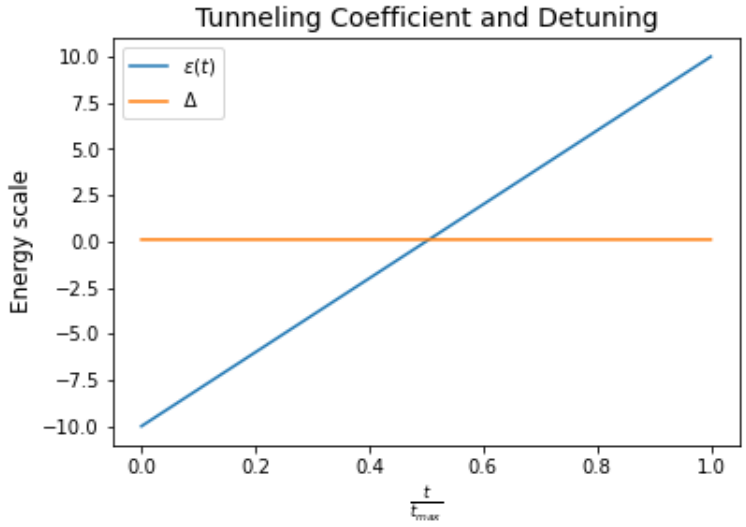

Figure 2: A plot showing the variation of the detuning, $\epsilon(t)$, and the tunnelling coefficient, Δ, with time. The tunnelling coefficient is held constant, $\Delta = 0.01$, while the detuning is ramped linearly, $\epsilon(t) \in [-10, 10]$. The two are equal at approximately $0.5t_{\max}$.

approximately equivalent, and evolve this state in time. We can then get the density matrix at

each moment and thus the populations of the states. For the diabatic states, the above analysis suggests that in the adiabatic limit we follow the solid red line in the right hand image of Figure (1) and thus our diabatic states will flip. So although we begin with a $|\uparrow\rangle$ state population of approximately 1, as $\epsilon(t)$ approaches and passes through Δ we should see the population of the $|\downarrow\rangle$ state become approximately 1 and the population of the $|\uparrow\rangle$ state become approximately 0. On the other hand, in the diabatic limit we follow the dashed red line in the right hand image of Figure (1) and our diabatic states remain the same, thus our populations should not change. This is exactly the behaviour we see in Figure (3).

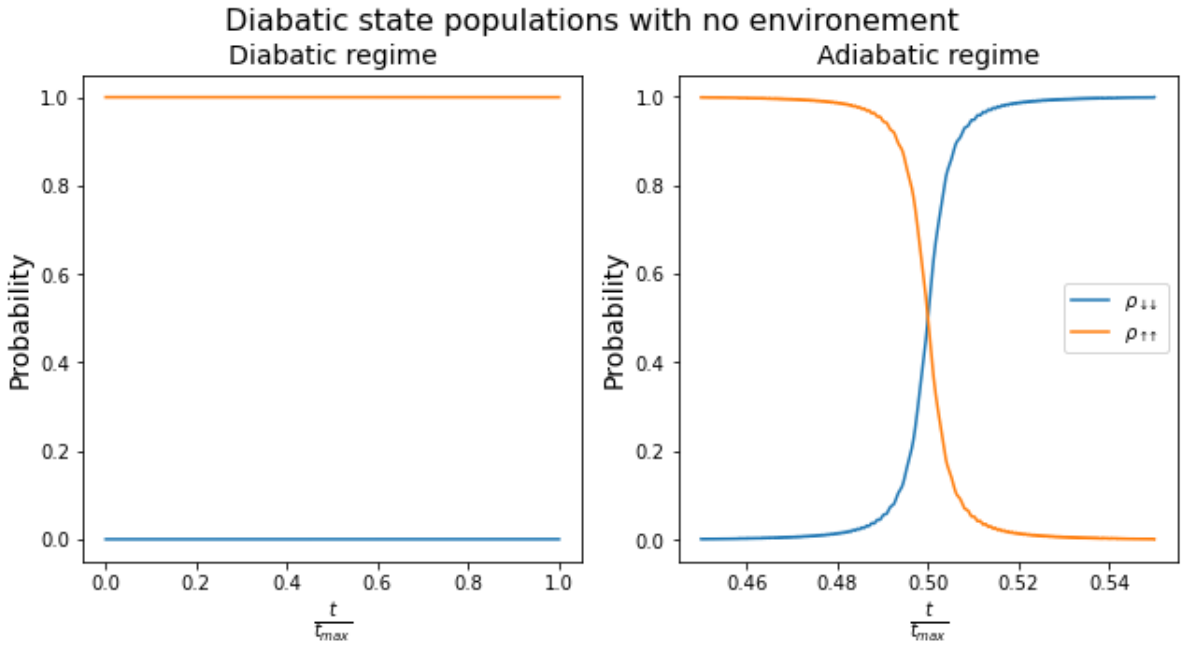

Figure 3: Two plots showing the populations of the diabatic basis states as we ramp the detuning, $\epsilon(t)$, diabatically (left), where $t_{\max} = 2$, and adiabatically (right), where $t_{\max} = 2 \times 10^4$, from -10 to 10. The tunnelling coefficient, Δ, is held at a small constant value of 0.01 and we only need consider 1 trajectory due to the lack on environment. For the adiabatic regime (right hand plot) we have narrowed the x-axis range around $t = 0.5t_{\max}$ to highlight the crossing.

We can consider the same scenario for the adiabatic states. Starting in the state $|-\rangle$, with negative $\epsilon(t)$, where $|\epsilon(t)| \gg \Delta$, an adiabatic increase should result in the state populations remaining the same while a diabatic increase should result in a basis flip, so the $|+\rangle$ state will become populated. This is shown in Figure (4).

We can now add back in the environment to see how it affects the system when we change parameters such as temperature, T, and system-environment coupling, α. The diabatic limit is no different from Figure (3) since the environment has no time to act. A regime with $t_{\max} = 200$ was chosen, which highlights the environment effects without the computational expense of the adiabatic limit. We consider the diabatic states, which will be relevant for our discussion on heat and work in Section (4). Figure (5) shows the diabatic state populations evolving in time when we take an ensemble average over 100 trajectories. The left hand plot shows the case of varying T and the right hand plot shows the case of varying α. We see that as we lower T and α the populations converge to the case where no environment is present.

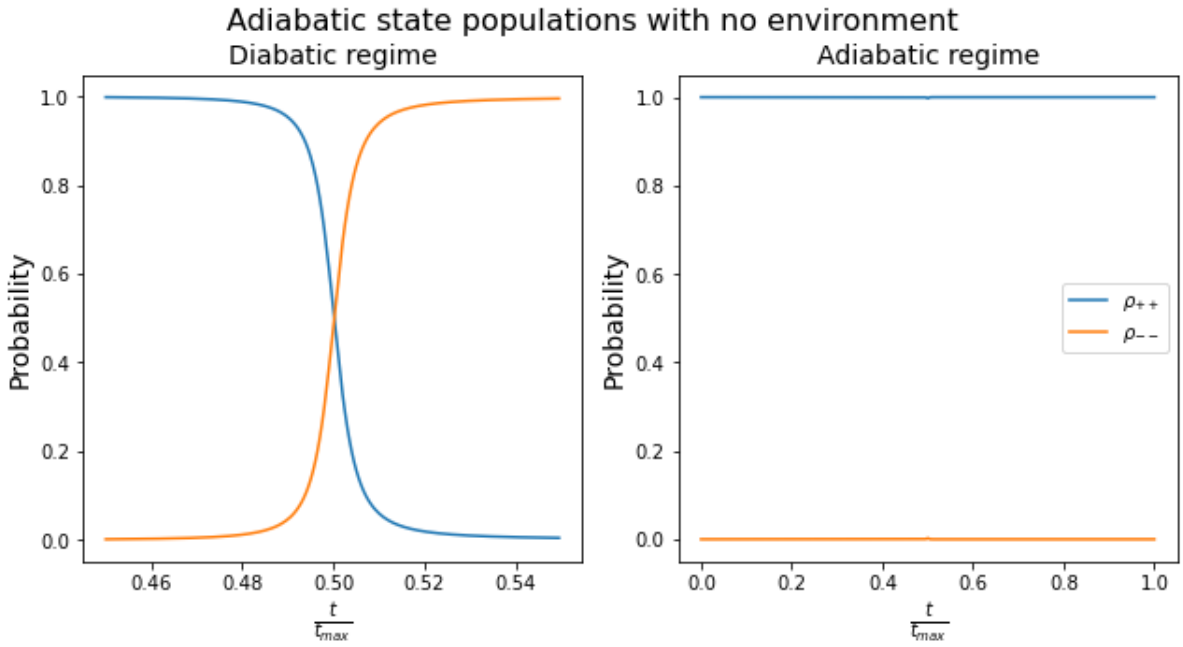

Figure 4: Two plots showing the populations of adiabatic states as we ramp the detuning, $\epsilon(t)$, diabatically (left), where $t_{\max} = 2$, and adiabatically (right), where $t_{\max} = 2 \times 10^4$, from -10 to 10. The tunnelling coefficient, Δ, is held at a small constant value of 0.01 and we only need consider 1 trajectory due to the lack on environment. For the diabatic regime (left hand plot) we have narrowed the x-axis range around $t = 0.5t_{\max}$ to highlight the crossing.

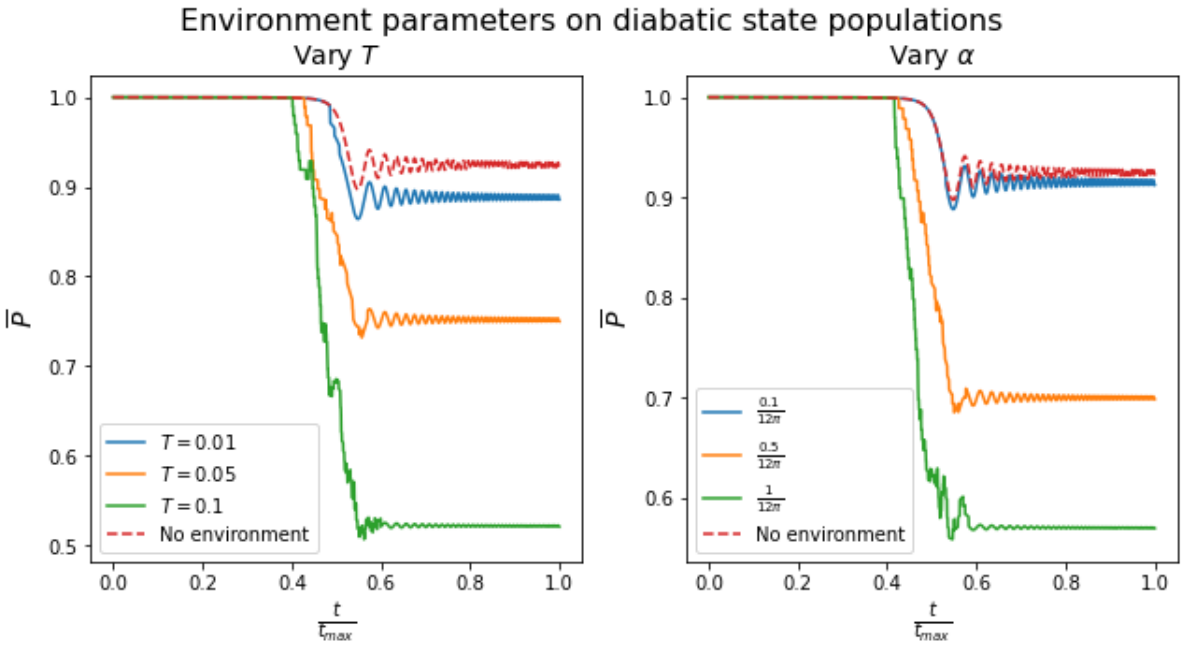

Figure 5: Two plots showing the population of $|\uparrow\rangle$ with time, when $t_{\max} = 2 \times 10^2$, and an environment is present. We average over 100 trajectories and ramp the detuning, $\epsilon(t)$, from -10 to 10 while holding the tunnelling coefficient, Δ, at a small constant value of 0.01. The left hand plot shows the effects of varying the temperature, T, where we set $\alpha = \frac{1}{12\pi}$ and the right hand plot shows the effects of varying the coupling strength, α, where we set $T = 0.1$.

3.2. The Landau-Zener formula

There exists an analytic solution for calculating transition probabilities in the absence of an environment, published separately by Landau and Zener in the early 1930s [5]. This only applies in the special case of a linearly changing perturbation where the time-dependent component does not couple our states, which is exactly the case we considered in Sub-section (3.1) where we linearly ramped $\epsilon(t)$ and held Δ constant.

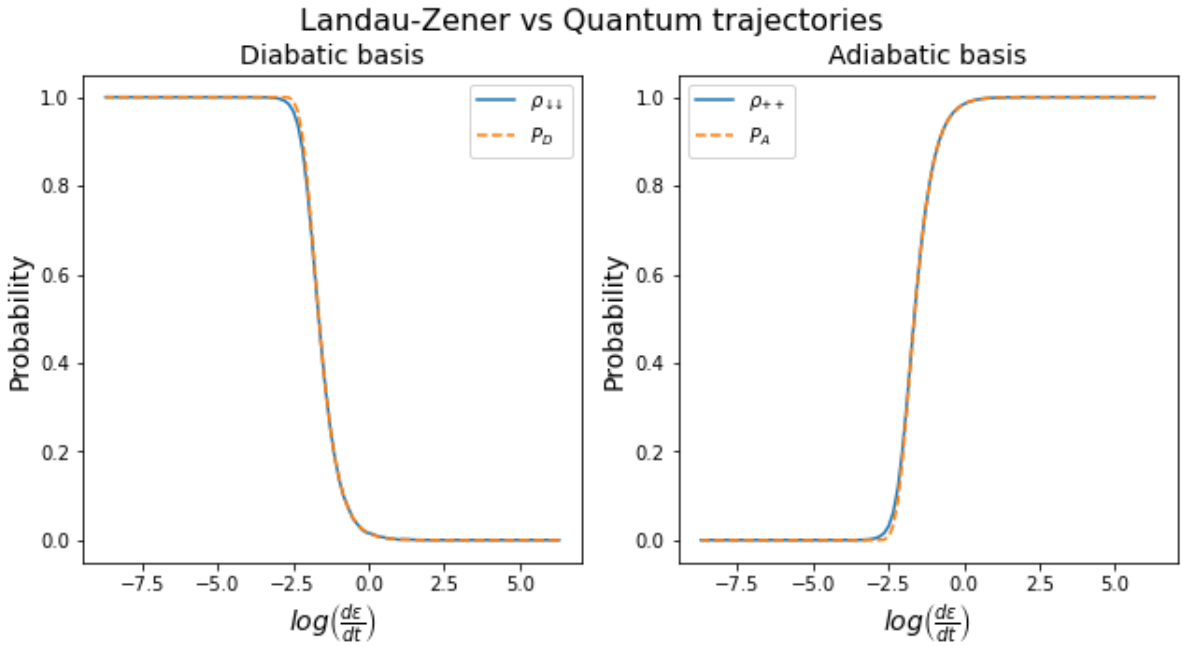

Figure 6: Two plots showing the probability for transition as given by the Landau-Zener formulas compared against the quantum trajectories result. In both plots we set $\Delta = 0.01$ and ramp $\epsilon(t)$ linearly at different speeds, always in the range -10 to 10 in order to start at a negative $\epsilon(t)$ and end with a positive $\epsilon(t)$ both satisfying $|\epsilon(t)| \gg \Delta$. We start in the adiabatic state $|-\rangle$ which at t_0 is approximately equivalent to the diabatic state $|\uparrow\rangle$. The x-axis is logarithmic in the gradient of the $\epsilon(t)$ ramp, so the far right represents the diabatic limit, where $t_{\max} = 2 \times 10^{-2}$, and the far left represents the adiabatic limit, where $t_{\max} = 2 \times 10^{4}$. The left hand plot is done in the context of the diabatic states and thus shows the Landau-Zener probability to observe such a diabatic transition, as given by equation (3.2.1), alongside the population of the $|\downarrow\rangle$ state. The right hand plot is done in the context of the adiabatic states and thus shows the Landau-Zener probability for a adiabatic transition, given by equation (3.2.3), alongside the population of the $|+\rangle$ state.

The Landau-Zener formula states the probability of a diabatic transition, i.e. following the dashed lines of Figure (1), is given by [5, p; 700]

$$P_D = 1 - e^{-2\pi\Gamma}, \tag{3.2.1}$$

where Γ is defined to be [5, p; 700]

$$\Gamma = \frac{\Delta^2}{\left|\frac{d\epsilon(t)}{dt}\right|}. \tag{3.2.2}$$

The probability for an adiabatic transition, i.e. following the solid lines of Figure (1) is then simply

$$P_A = e^{-2\pi\Gamma}. \tag{3.2.3}$$

We can thus vary $\epsilon(t)$ at different speeds and compare equations (3.2.1) and (3.2.3) to the relevant state population, where given our analysis in Sub-section (3.1) we should observe different results when working in either the diabatic or adiabatic basis. Figure (6) shows two plots, where the left hand plot is done in the context of the diabatic basis and the right hand plot in the context of the adiabatic basis. In both plots we consider a symmetric ramp of $\epsilon(t)$, starting from a negative value, where $|\epsilon(t)| \gg \Delta$, to a positive value obeying the same condition, hence forth known as a Landau-Zener style transition. Thus starting in the $|-\rangle$ state is approximately equivalent to the $|\uparrow\rangle$ state at t_0. The x-axis of this plot is logarithmic in the gradient of the ramp so the far left represents an adiabatic regime and the far right is the diabatic regime. For the diabatic basis (left hand plot) we observe that the $|\downarrow\rangle$ state is populated in the adiabatic regime, i.e. we experience a basis flip, and not in the diabatic regime, i.e. no basis flip occurs. This matches up to the Landau-Zener probability for a diabatic transition as in equation (3.2.1). For the adiabatic basis (right hand plot) we observe that the $|+\rangle$ state is populated in the diabatic regime, i.e. a basis flip has occurred, but not in the adiabatic regime, i.e. no flip occurs. This matches to the Landau-Zener probability for an adiabatic transition as in equation (3.2.3). This analysis is consistent with that of Sub-section (3.1).

4. Thermodynamic considerations and applications

Having now generalised the quantum trajectories method to incorporate a time-dependence, we wish to investigate various thermodynamic quantities such as heat, work and entropy and their applications to areas such as quantum computing.

4.1. Quantum logic gates

Two-level systems, such as the one we have considered up until now, have various applications, but one of the best known is to quantum computing, where they take the form of qubits. Physically a qubit could represent any two-level system that can be manipulated, for example an electron with two spin states which we can control by subjecting it to an external magnetic field with variable field strength. This is analogous to the ramping of $\epsilon(t)$ that we considered in Section (3).

The diabatic basis states, $|\uparrow\rangle$ and $|\downarrow\rangle$, label the spin-up and spin-down states of our qubit respectively. In quantum computing, we look to manipulate these states through quantum logic gates. The simplest operation is that of an X-gate, the quantum equivalent of a NOT-gate, which maps the state $|\uparrow\rangle \rightarrow |\downarrow\rangle$ and $|\downarrow\rangle \rightarrow |\uparrow\rangle$ [6, p; 18]. We can thus draw a direct parallel between the operation of such a gate and an adiabatic transition.

We wish to investigate how the work needed to achieve such a spin flip will change with the regime speed. The more real-world scenario of including an environment introduces extra complications due to heat transfer which we will shall consider. Ultimately it might be interesting to know the parameters which would minimise the work needed to perform these quantum logic gate operations.

4.2. Work

Initially we exclude the environment from our considerations so that no quantum jumps are taking place and thus there is no heat exchange. We are ramping the value of $\epsilon(t)$ so there is some work being done, whether that be by us or the system. The system Hamiltonian in the adiabatic basis can be shown to be

$$H_S = \frac{\eta(t)}{2} \left(|+\rangle \langle +| - |-\rangle \langle -| \right), \tag{4.2.1}$$

using the definitions in equations (2.1.19) and (3.1.1). With no environment present, the work done is simply the change in system energy over the trajectory, which is the trace of equation (4.2.1) with the final state, subtract the trace with the initial state.

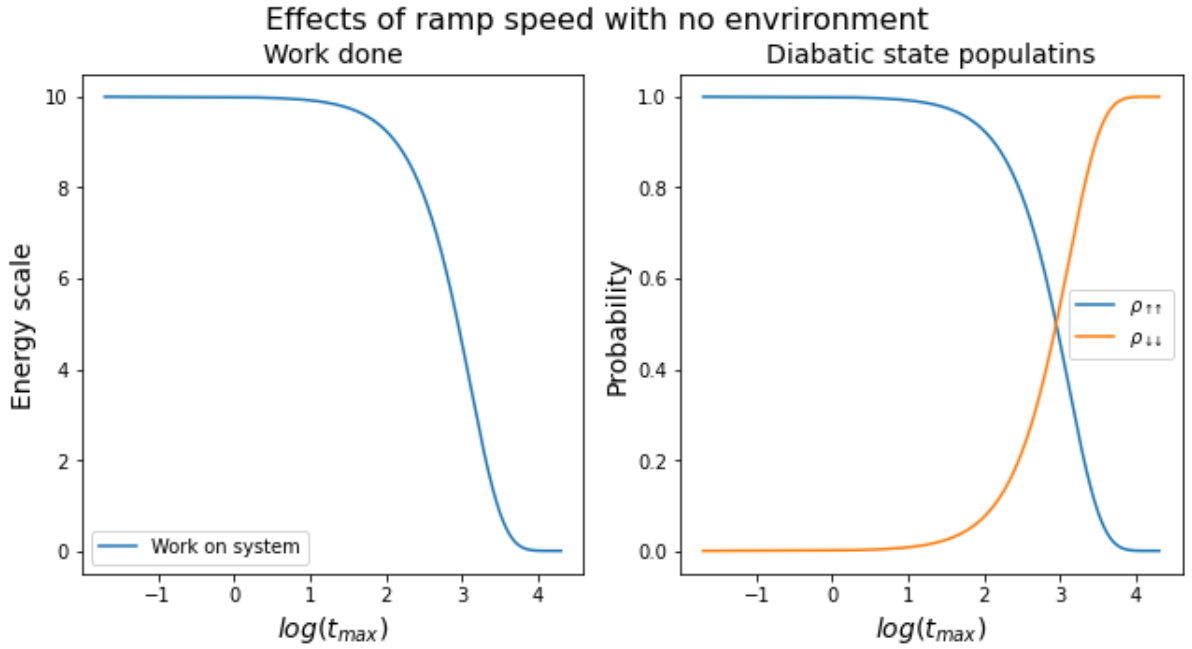

Figure 7: Two plots showing the effects of ramp speed when no environment is present. We consider a Landau-Zener style transition where the detuning is ramped linearly, $(t) \in [-10, 10]$ and the tunnelling coefficient is held at a small constant value, $\Delta = 0.01$. We start in $|-\rangle$ which approximately corresponds to $|\uparrow\rangle$ at t_0. The x-axis is logarithmic in the simulation time, so the regime on the left is diabatic, with $t_{\max} = 2 \times 10^{-2}$, and moves to adiabatic on the right, with $t_{\max} = 2 \times 10^{4}$. The left hand plot shows the work done to be zero in the adiabatic limit and finite in the diabatic limit which is consistent with the analysis in Sub-section (4.2). The right hand plot shows the population of the spin states where we see that in the adiabatic limit we observe a switch $|\downarrow\rangle$, whereas in the diabatic limit the basis does not flip and $|\uparrow\rangle$ remains populated as expected from the analysis of Sub-section (3.1).

We work in the adiabatic basis and consider a Landau-Zener style transition starting in the state $|-\rangle$, which is approximately equivalent to the state $|\uparrow\rangle$ at t_0. In the adiabatic limit we expect to remain in the $|-\rangle$ state, but for our spin state to flip to $|\downarrow\rangle$. The work done over the trajectory is

$$\begin{aligned} W_A &= \langle -| H_S(t_{max}) |-\rangle - \langle -| H_S(t_0) |-\rangle, \\ &= -\frac{\eta_-(t_{max})}{2} + \frac{\eta_-(t_0)}{2} = 0, \end{aligned}$$

This makes logical sense as we do some work increasing the energy of $|-\rangle$ as we ramp $\epsilon(t)$ from a large negative value to zero, and then as $\epsilon(t)$ is increased from zero to a large positive value, the system gives us an equal amount of work back as the energy of $|-\rangle$ decreases. Pictorially we are moving along the solid red line of the right hand image of Figure (1).

In the diabatic regime, we expect to switch to the $|+\rangle$ state, while the spin state remains $|\uparrow\rangle$. The work done in this case is

$$\begin{aligned} W_D &= \langle +| H_S(t_{max}) |+\rangle - \langle -| H_S(t_0) |-\rangle , \\ &= \frac{\eta_+(t_{max})}{2} + \frac{\eta_-(t_0)}{2} \equiv \eta \neq 0, \end{aligned}$$

i.e. we do a finite amount of work while not even flipping the spin.

Since there is no environment here we can use the Landau-Zener formula, equation (3.2.1), to determine the final spin state for different ramp speeds and then calculate the work done. Figure (7) shows two plots for the discussed scenario where the x-axis is logarithmic in the simulation time so that the far left represents the diabatic limit and the far right represents the adiabatic limit; a common theme moving forward. The left hand plot shows the amount of work we do, which is maximised in the diabatic limit and zero in the adiabatic limit. The right hand plot shows the populations of the spin states where we see that the spin state is flipped in the adiabatic limit but not in the diabatic limit as expected from our analysis in Sub-section (3.1).

4.3. Heat

Our analysis in Sub-section (4.2) suggested that if there was no environment present, and our goal is to flip the spin-state for the minimum amount of work, then an adiabatic regime is optimal. Adding the environment back in complicates the picture slightly as there is now the potential for quantum jumps to occur leading to heat dissipation and potential excitation of our system out of its ground state. So we could end up in scenarios where we are doing a finite amount of work or not flipping the spin-state as well in the adiabatic limit. We saw example of this in Figure (5) where the spin state population diverged from the no environment case when T and α were increased.

In theory a quantum jump would be instantaneous, but numerically it takes one time-step to occur. The total system energy change over a single time-step, when a jump occurs, is

$$\begin{aligned} E_{\text{jump}} &= \langle \pm| H_S(t + dt) |\pm\rangle - \langle \mp| H_S(t) |\mp\rangle , \\ &= \pm\frac{\eta(t + dt)}{2} \pm \frac{\eta(t)}{2}. \end{aligned}$$

This energy must be partitioned into heat and work which leads to us adopting the convention of evaluating the work with respect to the final state, while changing H_S by one time-step,

$$\begin{aligned} W_{\text{jump}} &= \langle \pm| H_S(t + dt) |\pm\rangle - \langle \pm| H_S(t) |\pm\rangle , \\ &= \pm\frac{\eta(t + dt)}{2} \mp \frac{\eta(t)}{2}, \end{aligned}$$

and then evaluating the heat by changing the state but keeping the Hamiltonian fixed,

$$\begin{aligned} H_{\text{jump}} &= \langle \pm | \, H_S(t) \, | \pm \rangle - \langle \mp | \, H_S(t) \, | \mp \rangle \,, \\ &= \pm \frac{\eta(t)}{2} \pm \frac{\eta(t)}{2} = \pm \eta(t). \end{aligned} \tag{4.3.1}$$

Of course, when no jump occurs we have a scenario similar to before, where the heat is zero,

$$H_{\text{no jump}} = \langle \pm | \, H_S(t) \, | \pm \rangle - \langle \pm | \, H_S(t) \, | \pm \rangle = 0,$$

and all the energy is in the work,

$$\begin{aligned} W_{\text{no jump}} &= \langle \pm | \, H_S(t+dt) \, | \pm \rangle - \langle \pm | \, H_S(t) \, | \pm \rangle \,, \\ &= \pm \frac{\eta(t+dt)}{2} \mp \frac{\eta(t)}{2} = E_{\text{no jump}}. \end{aligned}$$

It is easiest to calculate the total system energy change over the entire trajectory, as this is a single calculation, and then simply subtract the cumulative heat exchange from each quantum jump, given by equation (4.3.1). The difference is then the work done.

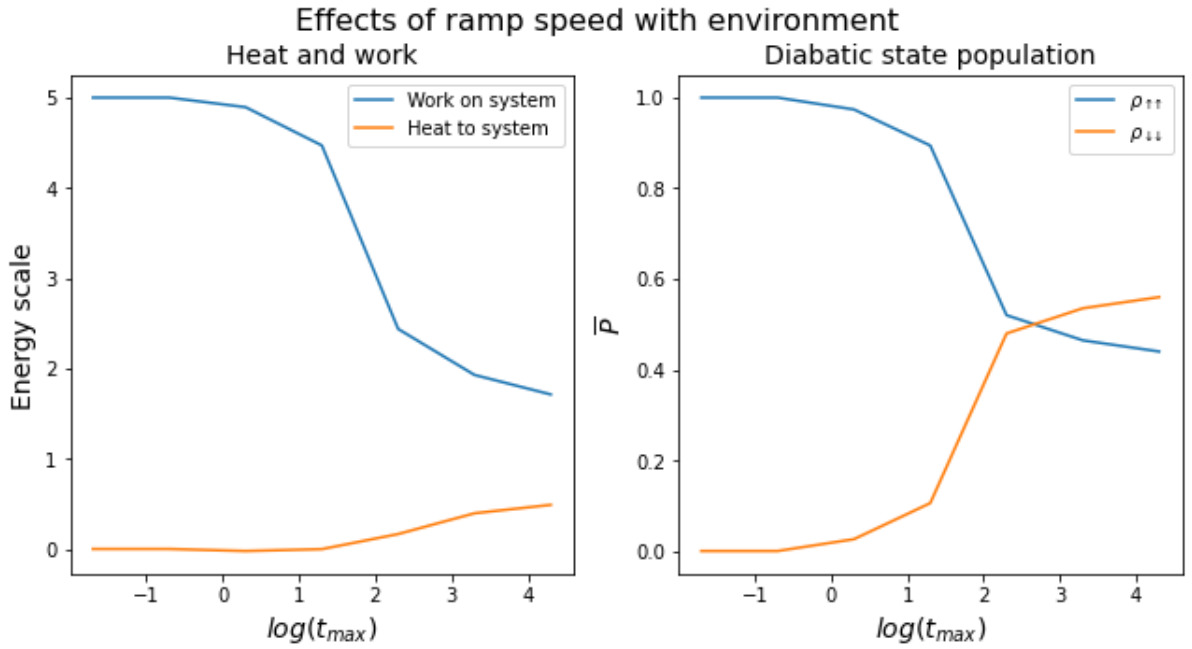

Figure 8: Two plots showing the effects of ramp speed in the presence of an environment, with $T = 0.1$ and $\alpha = \frac{1}{12\pi}$, for a Landau-Zener style transition where we linearly increase $\epsilon(t) \in [-10, 10]$ and fix $\Delta = 0.01$. Due to the presence of the environment we have to take an ensemble average over the trajectories and choose to use 40 to minimise the computational expense. The left hand image shows the cumulative heat and work done in each regime while the right hand plot shows the final spin-state having started in a state close to $|\uparrow\rangle$. The x-axis is logarithmic in the simulation length, so the regime is diabatic on the left, with $t_{\text{max}} = 2 \times 10^{-2}$, and moves to an adiabatic one, $t_{\text{max}} = 2 \times 10^{4}$, on the right.

Figure (8) shows the effects of varying the regime speed in the presence of an environment with temperature $T = 0.1$ and $\alpha = \frac{1}{12\pi}$. As usual we consider a Landau-Zener style transition

where we ramp the detuning, $\epsilon(t) \in [-10, 10]$, and fix the tunneling coefficient, $\Delta = 0.01$. We start all simulations in $|-\rangle$ which approximately corresponds to the spin-state $|\uparrow\rangle$ at t_0. Thus, we can make direct comparisons to Figure (7), where an environment was not present. In the diabatic regime no heat is transferred, since no quantum jumps occur as the environment does not have long enough to act, and we observe a diabatic transition where the spin-state does not flip. This is identical to the diabatic scenario without an environment. However, in the adiabatic limit, we observe some differences. Firstly, the spin is no longer as well flipped, we now finish in a mixed state rather than an almost pure $|\downarrow\rangle$ state as before, and we have to do a finite amount of work to achieve this. This is because we are not getting back the work that we initially put in as it is dissipated as heat which leads to only a partial spin flip. Regardless, we still find that the adiabatic regime is optimal as it is the regime that flips the spin the most, for the least amount of work. Since a quantum jump in our model takes a finite time we expect there to be a limit on how adiabatic our regime needs to be to get the best result.

We could change parameters such as environment temperature, T, or system-bath coupling strength, α, to get better results. As we saw at the end of Sub-section (3.1), the lower these quantities the more we approach the case of no environment which we know to be optimal scenario from Sub-section (4.2).

4.4. Entropy

We have seen in Sub-section (4.3) that in the presence of a finite temperature environment we always do a non-zero amount of work to partially flip the spin, even in the infinitely adiabatic regime. This is because some of the work we do in ramping $\epsilon(t)$ is not returned due to being dissipated as heat. The process is thus irreversible and therefore must have an associated entropy production [18, pp; 3-4].

The entropy balance equation, for the entropy production rate, $\sigma(t)$, in an open quantum system, is given by [19, p; 3]

$$\sigma(t) = \frac{dS(t)}{dt} + J(t), \tag{4.4.1}$$

where S is the von-Neumann entropy of the open system, defined as

$$S(t) = -k_B \mathrm{Tr}\left[\rho(t) \ln\left(\rho(t)\right)\right], \tag{4.4.2}$$

and $J(t)$ is the entropy flux, i.e. the entropy that flows per unit time from the open system to the environment, $J(t) > 0$, or from the environment to the open system, $J(t) < 0$.

To motivate the expression for the entropy flux $J(t)$, we recall that, by the quantum trajectory method, the environment causes the wave-function to undergo spontaneous quantum jumps, transferring energy $\omega(t)$. Since we previously assumed that the environment is in thermal equilibrium with the system at temperature T, the entropy change associated with a single quantum jump is simply

$$\delta S(t) = \frac{\omega(t)}{T}. \tag{4.4.3}$$

Now, the process $N^{\pm}(t)$ represents the amount of up and down quantum jumps within the time period $[0, t]$. Thus, the average amount of entropy flowing into the environment is

$$\frac{\omega(t)}{T} E\left[N^{-}(t) - N^{+}(t)\right]. \tag{4.4.4}$$

The derivative of equation (4.4.4) with respect to time yields the entropy flux,

$$J(t) = \frac{\omega(t)}{T}\frac{d}{dt}E\left[N^{-}(t) - N^{+}(t)\right]. \tag{4.4.5}$$

Now we can express equation (4.4.1) in the form

$$\sigma(t) = \frac{dS(t)}{dt} + \frac{\omega(t)}{T}\frac{d}{dt}E\left[N^{-}(t) - N^{+}(t)\right] \tag{4.4.6}$$

Figure (9) shows plots for the magnitudes of entropy flux (left) and von-Neumann entropy production rate (right) as we vary the regime in the adiabatic basis. In the diabatic limit the environment has little time to act and thus no quantum jumps occur, so the entropy flux is zero. For the adiabatic basis, we transition between basis states, but these states are pure and so we also see no von-Neumann entropy production. As we slow the regime the environment has enough time to induce jumps and we end in a mixed state, with both a finite J and $\frac{dS}{dt}$. The maximum rates are observed at faster regimes since even a small amount of total entropy produced manifests itself as a large rate due to the speed of the regime. As we move to the adiabatic limit, we expect more jumps to be occurring and the final state to be more mixed hence J and $\frac{dS}{dt}$ should increase. However, we see the rates decay to zero as the additional production does not offset the speed of the ramp itself. There will be a time where the environment has maximum potential to cause jumps, beyond which no more will occur, hence there is a maximum amount of total entropy that is ever produced and so ultimately we expect the production rates to always decay to zero.

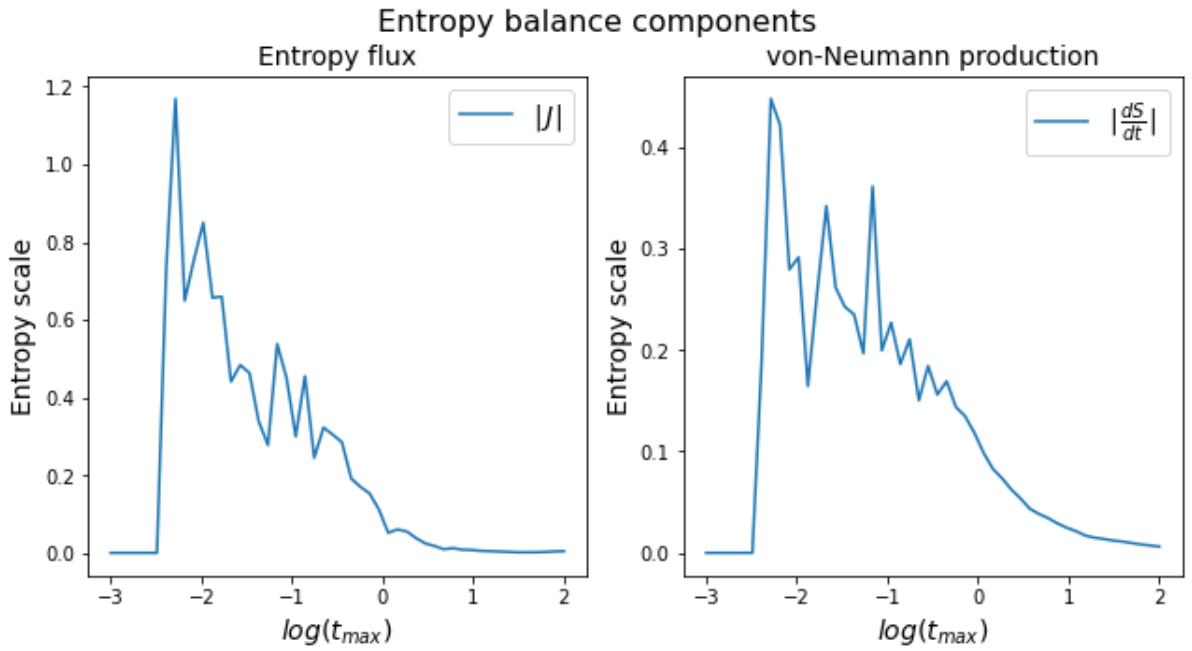

Figure 9: Two plots showing the magnitude of the components of the entropy balance equation. The left hand plot shows the entropy flux, J, and the right hand plot shows the von-Neumann entropy production rate, $\frac{dS}{dt}$. The x-axis is logarithmic in the simulation time so the far left represents the diabatic regime, with $t_{\max} = 2 \times 10^{-3}$, and the far right represents a more adiabatic regime, with $t_{\max} = 2 \times 10^{2}$. An environment is present with temperature $T = 0.1$ and coupling strength $\alpha = \frac{1}{12\pi}$, hence we take an ensemble average over 1×10^{4} trajectories.

5. Conclusion

We began the project by re-capping the mathematical formalism of density operators and Markovian master equations required for describing open quantum systems. To solve such equations we utilised the method of quantum trajectories which reduces the complexity of the problem in exchange for a statistical ensemble. Here we have generalised the procedure for the more realistic case of a time dependent Hamiltonian where we focused on Landau-Zener style transitions. Initially we investigated how ramping this energy at different speeds results in a basis state flip when we work in different bases, namely the z/diabatic-basis and the energy/adiabatic-basis. For the case of no environment we were able to directly compare our results from the quantum trajectories method to the analytic Landau-Zener formulas. Once we re-introduced the environment, the occurrence of quantum jumps disturbed the flipping of the basis states and we demonstrated the effects of changing environment parameters such as temperature and coupling strength. This lead us to studying thermodynamic quantities such as work, heat and entropy. Specifically we worked in the context of quantum logic gates where we looked to see how different regimes altered our ability to replicate such gates. We found that the case of no environment and infinitely slow ramp was preferable as we could achieve a spin flip without doing any work. The introduction of an environment lead to heat dissipation and we found we had to do a finite amount of work to flip the spin less well. Ultimately, lowering the temperature or coupling strength would improve the result. Finally, we identified that there must be an associated entropy production as the process was irreversible and demonstrated how its components changed during different regimes.

What we were able to achieve in the project was partially limited by the amount of computational power available to us. One of the biggest advantages of the quantum trajectories method is the ability to parallelise the process. This does not resolve the expense of adiabatic calculations but would potentially allow for better exploration of different regimes. It would be interesting to explore the idea of quantum logic gates further by considering different types of gates, potentially going beyond a two-level system and generalising to higher dimensions.

6. Length and date

The number of words in this document is 5162
This document was submitted on 23/05/21 at 14:30

References

[1] J. Von Neumann, "Wahrscheinlichkeitstheoretischer aufbau der quantenmechanik," *Nachrichten von der Gesellschaft der Wissenschaften zu Göttingen, Mathematisch-Physikalische Klasse*, vol. 1927, pp. 245–272, 1927.

[2] D. A. Lidar, "Lecture notes on the theory of open quantum systems," *arXiv preprint arXiv:1902.00967*, 2019.

[3] K. Mølmer, Y. Castin, and J. Dalibard, "Monte carlo wave-function method in quantum optics," *JOSA B*, vol. 10, no. 3, pp. 524–538, 1993.

[4] L. D. Landau, "Zur theorie der energieubertragung ii," *Z. Sowjetunion*, vol. 2, pp. 46–51, 1932.

[5] C. Zener, "Non-adiabatic crossing of energy levels," *Proceedings of the Royal Society of London. Series A, Containing Papers of a Mathematical and Physical Character*, vol. 137, no. 833, pp. 696–702, 1932.

[6] M. A. Nielsen and I. Chuang, "Quantum computation and quantum information," 2002.

[7] H.-P. Breuer, F. Petruccione, *et al.*, *The theory of open quantum systems*. Oxford University Press on Demand, 2002.

[8] J. J. Sakurai and E. D. Commins, "Modern quantum mechanics, revised edition," 1995.

[9] G. Schaller, *Open quantum systems far from equilibrium*, vol. 881. Springer, 2014.

[10] N. Chandra and R. Ghosh, "Quantum entanglement in electron optics," *Quantum Entanglement in Electron Optics: Generation, Characterization, and Applications*, p. 1, 2013.

[11] D. Manzano, "A short introduction to the lindblad master equation," *AIP Advances*, vol. 10, no. 2, p. 025106, 2020.

[12] D. Xu and J. Cao, "Non-canonical distribution and non-equilibrium transport beyond weak system-bath coupling regime: A polaron transformation approach," *Frontiers of Physics*, vol. 11, no. 4, p. 110308, 2016.

[13] J. F. Haase, A. Smirne, J. Kołodyński, R. Demkowicz-Dobrzański, and S. F. Huelga, "Fundamental limits to frequency estimation: a comprehensive microscopic perspective," *New Journal of Physics*, vol. 20, no. 5, p. 053009, 2018.

[14] C. Fleming, N. Cummings, C. Anastopoulos, and B. Hu, "The rotating-wave approximation: consistency and applicability from an open quantum system analysis," *Journal of Physics A: Mathematical and Theoretical*, vol. 43, no. 40, p. 405304, 2010.

[15] R. Dum, A. Parkins, P. Zoller, and C. Gardiner, "Monte carlo simulation of master equations in quantum optics for vacuum, thermal, and squeezed reservoirs," *Physical Review A*, vol. 46, no. 7, p. 4382, 1992.

[16] A. J. Daley, "Quantum trajectories and open many-body quantum systems," *Advances in Physics*, vol. 63, no. 2, pp. 77–149, 2014.

[17] T. Kato, "On the adiabatic theorem of quantum mechanics," *Journal of the Physical Society of Japan*, vol. 5, no. 6, pp. 435–439, 1950.

[18] S. R. De Groot and P. Mazur, *Non-equilibrium thermodynamics*. Courier Corporation, 2013.

[19] H.-P. Breuer, "Quantum jumps and entropy production," *Physical Review A*, vol. 68, no. 3, p. 032105, 2003.